PICOSECOND TIME SCALE OPTICAL COHERENCE EXPERIMENTS IN MIXED MOLECULAR CRYSTALS: PENTACENE IN NAPHTHALENE

D.E. COOPER, R.W. OLSON, R.D. WIETING and M.D. FAYER ‡
Department of Chemistry, Stanford University, Stanford, California 94305, USA

Received 19 March 1979; in final form 13 July 1979

Picosecond time scale high-power pulse optical coherence measurements including photon echo and the stimulated photon echo are obtained with a mode-locked dye laser synchronously pumped by a doubled Q-switched and mode-locked Nd:YAG laser. Effects on coherence arising from excitation with gaussian laser pulses rather than square pulses are examined. Preliminary echo decay measurements are reported.

1. Introduction

In the early 1950's, the development of high-power pulsed magnetic resonance techniques revolutionized magnetic resonance spectroscopy by providing direct methods for obtaining dynamical information, often in the only manner possible [1,2]. This class of experiments has a common theme. An rf pulse sequence is applied to establish a macroscopic oscillating magnetic dipole in the sample. This dipole arises from an in-phase (coherent) ensemble of superpositions of spin eigenstates induced by the rf field via the magnetic dipole transition matrix element. The information contained in the time dependence of the in-phase (coherent) component depends on the particular pulse sequence. For example, the "free induction decay" examines the time dependence of the coherent component induced by a single pulse. This experiment is the basis for Fourier transform NMR [2].

Today, the development of high-powered picosecond time scale pulsed optical coherence experiments has the potential to greatly alter the nature of optical spectroscopy by permitting the full range of techniques developed in magnetic resonance to be applied to optical systems on an appropriately fast time scale. Gibbs observed a photon echo on this time scale in a gas phase sample [3] using a pulsed method. Wiersma and co-workers in an elegant and extremely complex experiment observed the first picosecond time scale photon echo in a mixed molecular crystal [4]. On the other hand, low power optical coherence methods pioneered by Brewer and co-workers have already proven to be of great utility in certain systems and have been extended into the picosecond time regime [5]. However, the low power method is in general not capable of "turning over" the entire inhomogeneous optical absorption line. Thus the full range of experiments developed in magnetic resonance, such as the stimulated echo, is not accessible with the low power methods.

The purpose of this paper is threefold. First, differences between pulsed magnetic resonance experiments and picosecond time scale optical coherence experiments produced by the temporal shape of the optical pulses are discussed. Second, an experimental setup for performing high-powered picosecond time scale optical coherence experiments is described. In the original mixed crystal experiments two mode-locked dye lasers and four stages of nitrogen laser pumped dye amplifiers operating at 10 Hz were used [4]. The apparatus described here is based around a single high repetition rate (0.4 kHz) mode-locked dye laser of sufficient output (10 μJ/pulse) to avoid the necessity of amplification. The great reduction in experimental complexity afforded by this apparatus coupled with the high repetition rate results in excellent signal to

‡ Alfred P. Sloan Fellow and Dreyfus Foundation Fellow.

noise ratios from a system with the dependability and flexibility to perform a variety of experiments.

Experimental observations of two optical coherence experiments, the two-pulse photon echo and the three-pulse stimulated photon echo, are presented. The photon echo and the stimulated photon echo were detected by observing the coherent "superradiant" emission in the forward direction [6]. The stimulated echo is a pulse sequence designed to study spectral diffusion [7]. This experiment may prove valuable in answering recent questions pertaining to spectral diffusion in optical systems. Experimental data and a short discussion of the photon echo intensity dependence and a fluorescence detected transient nutation [8,9] are given. Finally, photon echo decay data are presented and preliminary findings are briefly discussed.

2. Theory — the adiabatic property in picosecond pulse optical coherence experiments

In order to treat the coherent evolution of an ensemble of identical two-level systems driven by an electric field oscillating at frequency ω, a semiclassical driving field hamiltonian is employed. The rotating field approximation is used and a transformation to a coordinate frame rotating at the frequency of the applied field is made [10]. The ensemble averaged properties of the system are contained in the time evolution of the density matrix $\rho(t)$, which is governed by [11]

$$\rho(t) = Q^{\dagger}\rho(0)Q, \tag{1}$$

where the time evolution operator Q is

$$Q = \exp(i\mathcal{H}t/\hbar). \tag{2}$$

$\mathcal{H}$ is the *time-independent* hamiltonian in the rotating frame and $\rho(0)$ is the initial state of the system when a given field is applied. $\mathcal{H}$ is a function of the amplitude of the driving field ω_1 ($\omega_1 = \boldsymbol{\mu}\cdot\boldsymbol{E}/\hbar$, where $\boldsymbol{\mu}$ is the electric dipole transition moment and $\boldsymbol{E}$ is the strength of the applied field) and $\Delta\omega$, the difference between ω and the resonant transition frequency ω_0. Eq. (1) applies to a single isochromat at ω_0, and the behavior of an inhomogeneously broadened absorption line is obtained by integrating $\rho(t)$ over the lineshape. This treatment is adequate to describe experiments in which the driving field amplitude is constant during the applied pulse, i.e. square pulse experiments and can be easily extended to pulse sequences via the application of additional transformations in eq. (1) employing operators Q representing field-free intervals and additional square pulses.

For a picosecond laser pulse, ω_1 is not constant during the pulse but rather a function such as a gaussian. To introduce the laser pulse shape into the problem, the temporal envelope is approximated by a histogram. In each slice of the histogram ω_1 is taken to be constant and therefore eq. (1) can be employed in a manner analogous to the square pulse sequence discussed above. The histogram is increasingly finely divided until the calculation converges.

It is convenient to use the Feynman et al. [10] vector model to describe the state of the optical system in terms of the vector r

$$r = (r_1, r_2, r_3). \tag{3}$$

r_3 represents the population difference between the ground and the excited state (equivalent to M_z, the net magnetization, in an NMR experiment). r_1 and r_2 represent the in-plane coherent components of the oscillating electric dipole (equivalent to M_x and M_y, the in-plane magnetization). The components of r are directly related to the elements of the density matrix. The density matrix equation of motion becomes a Bloch-like equation

$$\dot{r} = \boldsymbol{\omega}_e \times r, \tag{4}$$

where the effective driving field $\boldsymbol{\omega}_e$ is a vector sum of the applied driving field ω_1 and the $\Delta\omega$,

$$\boldsymbol{\omega}_e = (\omega_1, 0, \Delta\omega). \tag{5}$$

The transient nutation experiment [2] can be used to illustrate the differences between picosecond optical coherence experiments which employ fixed duration laser pulses and experiments employing the normal variable duration square pulses. In a fluorescence detected nutation experiment [8,9] r is made to precess via the application of a radiation field, and the final state of r_3 is monitored via the total integrated fluorescence. For the ensemble of molecules on resonance, i.e. $\Delta\omega = 0$, precession occurs around the applied field, $\boldsymbol{\omega}_1$, and the r_3 component varies as

$$r_3 \propto \cos\omega_1 t. \tag{6}$$

In a square pulse experiment the pulse duration, t, is varied. In the experiment using the picosecond pulse,

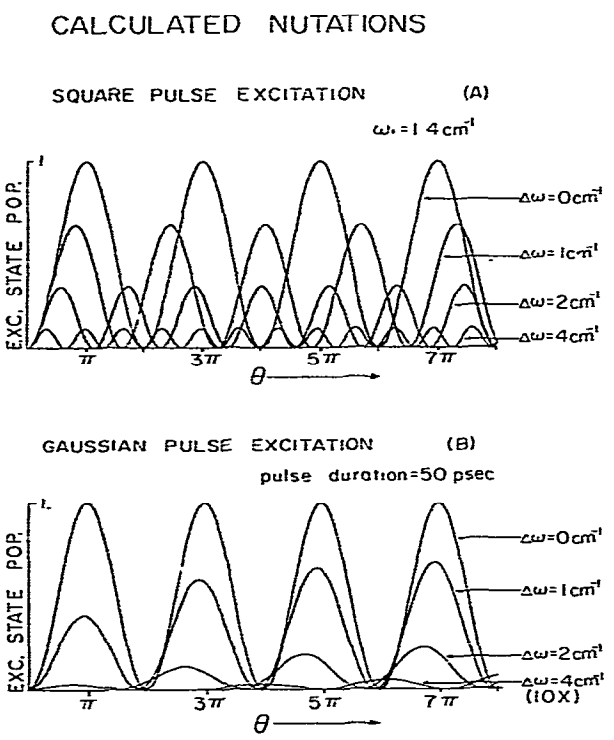

Fig. 1. Calculated excited state population of a single isochromat in an optical nutation experiment. Curves are for isochromats 0, 1, 2, and 4 cm^{-1} off resonance. (a) Square pulse excitation; ω_1 = 1.4 cm^{-1} and pulse duration is varied. (b) Gaussian pulse excitation; pulse fwhm = 50 ps and pulse intensity is varied. Note $\Delta\omega$ = 4 cm^{-1} curve is magnified 10 ×. All curves plotted versus θ, the on-resonance angle of precession.

the duration is fixed and ω_1 is varied, i.e. the intensity of the laser beam, $I \propto \omega_1^2$, is varied. From eq. (6) the two are equivalent.

For an isochromat off resonance, i.e. $\Delta\omega \neq 0$, the situation is different. Off resonance, r precesses around the effective field, $\boldsymbol{\omega}_e$ [2,10], with magnitude $\omega_e = [(\Delta\omega)^2 + \omega_1^2]^{1/2}$. For a square pulse $\boldsymbol{\omega}_e$ is constant in direction and magnitude since ω_1 is constant. However for a picosecond pulse, ω_1 increases continuously from zero to ω_1(max) and returns to zero. Thus the direction and magnitude of $\boldsymbol{\omega}_e = \boldsymbol{\omega}_1 + \Delta\boldsymbol{\omega}$ evolve during the pulse. As the peak laser intensity is increased, ω_1(max) is increased and therefore both the range of $\boldsymbol{\omega}_e$ covered and the rate of change of the $\boldsymbol{\omega}_e$ increases. If the rate of change of the $\boldsymbol{\omega}_e$ is not too great, r which is initially parallel to $\Delta\boldsymbol{\omega}$, remains approximately aligned with $\boldsymbol{\omega}_e$. The vector r is said to follow the field adiabatically [11]. In this situation a nutation effectively does not occur since r returns to its initial state at the end of the pulse. Whether the adiabatic condition is met depends on the pulse duration, $\Delta\omega$, and ω_1(max).

In fig. 1 nutation calculations for a single isochromat are displayed. The upper curves (fig. 1a) give the excited state population for square pulse excitation as the duration of the pulse is increased. The lower curves (fig. 1b) give the excited state population for gaussian pulse excitation as the peak intensity of the pulse is increased. Curves are shown for an isochromat on resonance, and 1 cm^{-1}, 2 cm^{-1}, and 4 cm^{-1} off resonance. The curves are plotted against θ ($\theta = \omega_1 t$), the precession angle of r for an on-resonance isochromat. As $\Delta\omega$ increases, the square pulse nutation rapidly increases in frequency. This effect is much less pronounced in the gaussian pulse nutation. For a fixed $\Delta\omega \neq 0$, the maximum excited state population increases with each cycle of the fixed duration gaussian pulse nutation since increased ω_1(max) will result in a greater rate of change of ω_1 breaking the adiabatic condition. The adiabatic limit is illustrated by the $\Delta\omega$ = 4 cm^{-1} curve in fig. 1b which displays virtually zero excited state population. This contrasts with the $\Delta\omega$ = 4 cm^{-1} square pulse nutation, fig. 1a, in which the maximum excited state population is ≈10%.

In a real system, there will be an inhomogeneous line with a continuous range of $\Delta\omega$. In fig. 2 nutation calculations are displayed for a gaussian inhomogeneous line. Square pulse excitation will tend to involve more of the inhomogeneous line but there are large spreads in nutation frequencies across the line, resulting in damping of the nutation oscillation. Gaussian pulse excitation may tend to leave the wings to a wide inhomogeneous line out of the experiment because of the adiabatic condition, but those isochromats which are involved will have nearly the same nutation frequency. Thus in an experiment requiring a well-defined pulse, for example a $\pi/2$ pulse in an echo sequence, gaussian pulse excitation can be readily employed.

3. Experimental

Tunable, high-power picosecond excitation pulses for the photon echo and stimulated photon echo exper-

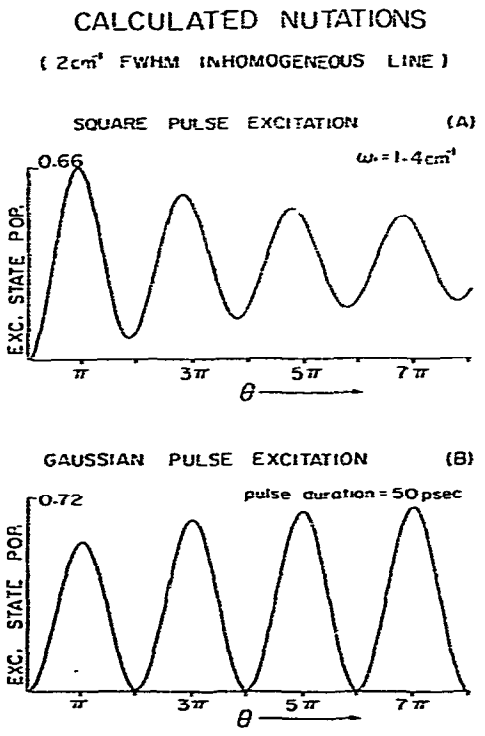

Fig. 2. Calculated excited state population for an inhomogeneous gaussian absorption line (fwhm = 2 cm^{-1}) in an optical nutation experiment. (a) Square pulse excitation. (b) Gaussian pulse excitation.

iments were produced by a cavity-dumped mode-locked dye laser synchronously pumped by a frequency-doubled, continuously pumped, acousto-optically Q-switched and mode-locked Nd:YAG laser. Operating at 0.4 kHz, the YAG laser [12] is a stable source of pulse trains consisting of 30 pulses of 80 ps duration and separated by 5.7 ns. Frequency-doubling in a temperature-tuned CD*A crystal resulted in green pulses of 60 ps duration and yielded pulse trains containing ≈300 μJ at 532 nm.

The dye laser cavity (fig. 3) consists of two 100% reflectors and an electro-optic cavity dumping system. The cavity length was matched to that of the YAG laser and adjusted for minimum pulse duration. The cavity dumping system consisted of a Pockels cell and a Glan–Thompson polarizer with escape window. The Pockels cell was switched with 1 ns rise time by a string of avalanche transistors triggered by dye laser pulse train leakage through one of the cavity mirrors,

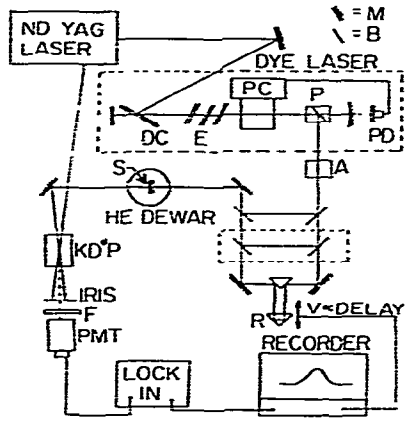

Fig. 3. High power, high repetition rate synchronously pumped picosecond dye laser and optical coherence experimental apparatus. A = attenuator, B = beamsplitter, DC = flowing dye cell, E = etalons, F = filter, M = mirror, P = Glan–Thompson polarizer, PC = Pockels cell, PD = photodiode, R = right-angle prism, S = sample with pinhole. The beamsplitters in the dashed box are used in the stimulated echo experiment only.

and a single pulse is deflected out of the cavity. The result is a high repetition rate (0.4 kHz) dye laser with sufficient output to perform a wide variety of optical coherence experiments without additional amplifier stages. For optical coherence experiments two etalons were introduced into the cavity to obtain transform limited pulses. 40 ps, 6 μJ pulses with a $\Delta\nu\Delta t$ product of 0.54 were used in the experiments.

The photon echo and stimulated echo observation experiments were performed on single crystals of 10^{-6} mole/mole pentacene in naphthalene at ≈2 K. The collimated laser beams were directed through a 400 μm diameter pinhole into the crystal (fig. 3). The dye laser single pulse tuned to the absorption origin (602.6 nm) was split into the appropriate two or three pulse sequence for the echo or stimulated echo, respectively, by a beam splitting network incorporating fixed delays and a variable delay for one of the pulses (fig. 3). For the photon echo the pulses were recombined collinearly with an energy ratio of 1:4 ($\pi/2$–π) [2] and a variable delay on the second pulse. For the stimulated echo two more beamsplitters were added to the beam-splitting network to obtain three collinear pulses of equal intensity ($\pi/2$–$\pi/2$–$\pi/2$) [7]. The echoes were detected by a nonlinear frequency mixing technique

[13,4]. After emerging from the sample the dye laser beam and the collinear echo were focused into a type II KD*P crystal and crossed with an IR pulse (1.06 μm) from the YAG pump laser. The crystal was angle tuned to generate the sum frequency. The signal was filtered with an iris and a UV bandpass filter, detected by a cooled EMI 6256B PMT and lock-in amplifier, and recorded on an $X-Y$ plotter. The cross-correlation function of the IR pulse with the echo is generated by scanning the motorized delay line, which also produces a voltage proportional to the optical delay.

In the photon echo decay experiments and stimulated photon echo decay experiments, the same basic setup is used. However, the optics are rearranged such that, as the motorized delay line is scanned, the separations between the pulses change in the appropriate manner. This experimental arrangement will be described in detail in a subsequent publication [15].

For the optical nutation experiment the optical pulses tuned to the absorption origin (592.2 nm) were directed into an $\approx 10^{-7}$ mole/mole pentacene in *p*-terphenyl single crystal at 2 K. Fluorescence from the sample was filtered to eliminate scattered laser light and detected by a phototube. The integrated photo current following each laser pulse was sampled by a sample-and-hold circuit and acquired by computer. Simultaneously the intensity of the dye laser pulse was monitored by a silicon PIN photodiode, sampled by another sample-and-hold circuit, and acquired by the computer. A data set was produced by slowly varying the excitation intensity while collecting data.

4. Results

In fig. 4a pentacene in naphthalene photon echo experimental results are displayed. As can be seen, the signal to noise ratio is excellent. In fact the signal was so strong that the photon echo was *attenuated by a factor of 1000* before it arrived at the PMT to prevent overload. The energy in the echo superradiant pulse was measured to be ≈0.1 nJ. The width and shape of the experimental curve is determined by the cross-correlation of what are basically back-to-back free induction decays with the IR detect pulse which has known shape and duration. Deconvolution yields the echo envelope.

In order to perform optically the wide variety of

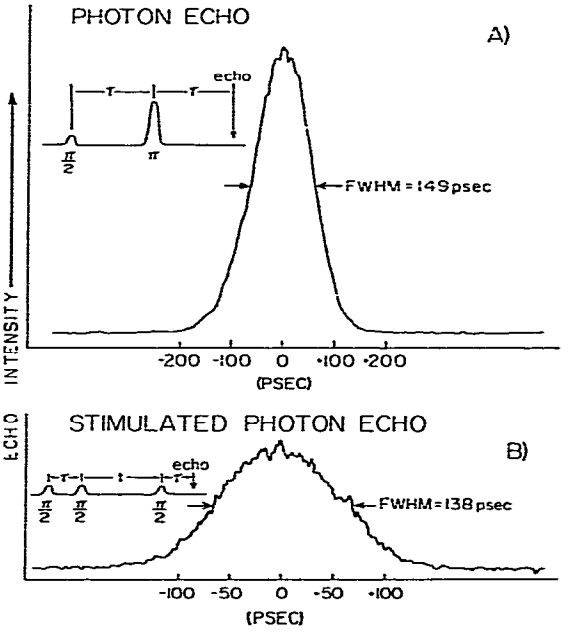

Fig. 4. (a) Photon echo signal of pentacene in naphthalene (2 K), detected in the forward direction. The data, which has excellent signal-to-noise, was obtained following a 10^3 optical attenuation of the echo pulse. (b) Stimulated photon echo signal of the same sample, which was also attenuated by 10^3.

experimental pulse sequences available to the magnetic resonance spectroscopist, it is necessary to have well defined $\pi/2$ and π pulses. In the echo experiment ($\pi/2-\pi$), the necessary 1:4 intensity ratio (1:2 in E field) is established and the total intensity is adjusted until the pulses have the correct magnitude as well as ratio. In fig. 5a the echo amplitude as a function of pulse intensity is shown. The arrow indicates where the maximum echo should occur based on the reported ≈1 debye oscillator strength [14] of the transition. This demonstrates the existence of well-defined $\pi/2$ and π pulses.

The echo intensity dependence indirectly detects a transient nutation by looking at the magnitude of the in-plane coherent component. A nutation can be detected by measuring the intensity of incoherent fluorescent emission as a function of the intensity of the excitation pulse. A fluorescent detected nutation has been observed in low power experiments using "square" pulses [9]. In a high powered nutation experiment the integrated fluorescence, proportional to the excited state population, should oscillate as the laser intensity

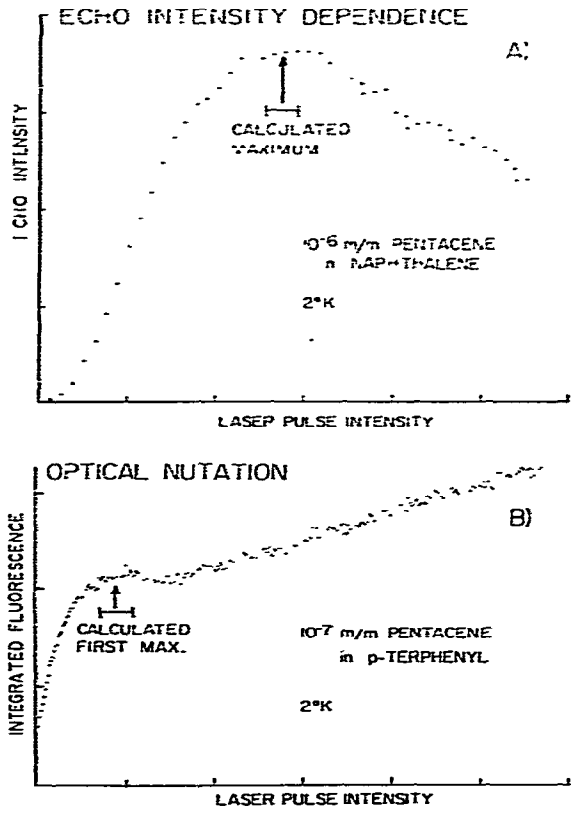

Fig. 5. (a) Intensity dependence of photon echo signal. Arrow indicates where maximum is predicted to occur. (b) Optical nutation experiment detected by incoherent fluorescent emission. Arrow indicates where first maximum is predicted to occur. Error bars below arrows indicates uncertainty in predicted maxima.

is increased (section 2 and figs. 1 and 2). Results of an attempted nutation experiment are shown in fig. 5b. The arrow indicates where the first maximum should occur based on an ≈1 debye pentacene oscillator strength. Although clearly suggestive, the results are not nearly as well-defined as in the echo power dependence due to a number of experimental problems involving scattered light and reflection off of the back surface of the crystal, which were difficult to overcome.

The results of the picosecond time scale stimulated photon echo experiments are shown in fig. 4b. As in the photon echo experiments, the optical signal was very strong and was attenuated by a factor of 10^3 for comparison with the echo results. The stimulated photon echo, like the stimulated spin echo of magnetic resonance, is capable of examining the time-dependence and the extent of spectral diffusion [7]. There are a variety of important physical processes such as changes in solvation in liquids or energy transport in mixed solids which can manifest themselves as spectral diffusion.

The experiments described above demonstrate that we can detect picosecond time scale photon echoes and stimulated photon echoes with excellent signal to noise. However, the important information is obtained from decay experiments. In an echo experiment the intensity is measured as a function of the time, 2τ, between the $\pi/2$ pulse and the echo (see inset, fig. 4a). The decay measurements yield the homogeneous T_2. Fig. 6 shows an echo decay curve taken on a 6×10^{-6} mole/mole pentacene in naphthalene crystal at 2.15 K. The signal to noise ratio is excellent. The decay is exponential and the homogeneous T_2 is 8.4 ns, considerably faster than would be produced by the lifetime alone. This is most likely due to concentration dependent intermolecular interactions between pentacene molecules. A preliminary theoretical analysis suggests that at short times there is a concentration dependent dephasing mechanism that does not involve energy transport. A calculation involving dipole interactions and an ensemble average over intermolecular separations closely simulates experimental results without

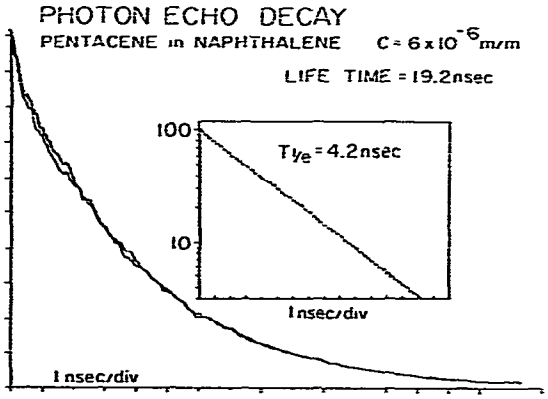

Fig. 6. Photon echo decay as a function of 2τ. Two experimental scans are shown to demonstrate the reproducibility of the data. The decay is exponential (see inset) and gives a homogeneous T_2 of 8.4 ns, which is considerably shorter than if it were determined by the excited state lifetime alone.

recourse to adjustable parameters. The theoretical and experimental results demonstrate that concentration dependent effects are negligible in this system at concentrations of 10^{-7} mole/mole or lower.

To examine the low concentration limit, measurements were made on six different crystals of $\approx 10^{-7}$ mole/mole concentration at 2.14 K and below. T_1 was obtained by fluorescence decay measurements on $\approx 10^{-9}$ mole/mole crystals at ≈ 2 K and is 19.2 ns. The preliminary results demonstrate that T_2 is not determined solely by T_1, the excited state lifetime. For example, at 2.14 K $T_2 = 28$ ns instead of 38.4 ns which would result from the lifetime. Temperature dependent studies of T_2 between 2.14 K and 1.4 K suggest a dephasing mechanism involving acoustic phonons since the non-lifetime component of T_2 has a "pseudo-activation energy" of less than 4 cm^{-1} and the temperature dependence appears to be non-exponential. The mechanism may involve acoustic phonon induced density fluctuations which modulate the molecular excited state site energy by causing fluctuations in the ground state and excited state van der Waals interactions [15]. A detailed account of the concentration and temperature dependent results will be presented in subsequent publications [16].

Acknowledgement

We would like to thank Wm. Fayer for invaluable assistance with electronic engineering and other aspects of these experiments. This work was supported by the National Science Foundation, Division of Materials Research Grant DMR76-22019.

References

[1] J.S. Waugh, C.H. Wang, L.M. Huber and R.L. Vold, J. Chem. Phys. 48 (1968) 662.
[2] T.C. Farrar and E.D. Becker, Pulse and Fourier transform NMR (Academic Press, New York, 1971).
[3] H.M. Gibbs and P. Hu, in: Picosecond phenomena, eds. C.V. Shank, E.P. Ippen and S.L. Shapiro (Springer, Berlin, 1978).
[4] W.H. Hesselink and D.A. Wiersma, Chem. Phys. Letters 56 (1978) 227.
[5] R.G. Brewer, in: Frontiers in laser spectroscopy, Vol. 1, Les Houches, eds. R. Balian, S. Haroche and S. Liberman (North-Holland, Amsterdam, 1977);
R.G. DeVoe and R.G. Brewer, Phys. Rev. Letters 40 (1978) 862.
[6] I.D. Abella, N.A. Kurnit and S.R. Hartmann, Phys. Rev. 141 (1966) 391.
[7] W.B. Mims, in: Electron paramagnetic resonance, ed. S. Geschwind (Plenum Press, New York, 1972) ch. 4.
[8] W.G. Breiland, H.C. Brenner and C.B. Harris, J. Chem. Phys. 62 (1975) 3458.
[9] T.E. Orlowski, K.E. Jones and A.H. Zewail, Chem. Phys. Letters 50 (1977) 45.
[10] R.P. Feynman, F.L. Vernon Jr. and R.W. Hellwarth, J. Appl. Phys. 28 (1957) 49.
[11] C.P. Slichter, Principles of magnetic resonance (Harper and Row, New York, 1963).
[12] D.J. Kuizenga and A.E. Siegman, IEEE J. Quantum Electron. QE-6 (1970) 694, 709.
[13] H. Mahr and M.D. Hirsch, Opt. Commun. 13 (1975) 96.
[14] H. de Vries, P. de Bree and D.A. Wiersma, Chem. Phys. Letters 52 (1977) 399;
H. de Vries and D.A. Wiersma, J. Chem. Phys. 69 (1978) 897;
T.E. Orlowski, K.E. Jones and A.H. Zewail, Chem. Phys. Letters 54 (1978) 197;
T.E. Orlowski and A.H. Zewail, J. Chem. Phys. 70 (1979) 1390.
[15] K.A. Nelson and M.D. Fayer, J. Chem. Phys., to be published.
[16] D.E. Cooper, R.W. Olson and M.D. Fayer, J. Chem. Phys., to be published.